Int. J. Heat Mass Transfer. Vol. 13, pp. 689–702. Pergamon Press 1970. Printed in Great Britain

EXPERIMENTS ON HYDRODYNAMICALLY DEVELOPING FLOW IN RECTANGULAR DUCTS OF ARBITRARY ASPECT RATIO

G. S. BEAVERS, E. M. SPARROW and R. A. MAGNUSON

School of Mechanical and Aerospace Engineering, University of Minnesota, Minneapolis, Minnesota, U.S.A.

(*Received* 4 *August* 1969 *and in revised form* 19 *September* 1969)

Abstract—A comprehensive experimental investigation of laminar flow development in rectangular ducts is performed employing an apparatus which permits study of any cross sectional aspect ratio. The primary concern of the research is the determination of the pressure field associated with the hydrodynamic development of the flow. Experimental results are presented in terms of both the local pressure defect and the incremental pressure drop due to flow development. Comparisons are made with the available predictions of analysis and with prior experimental information. Hydrodynamic development lengths are deduced and the threshold of significant effects of the viscous normal stress is identified.

NOMENCLATURE

A,	aspect ratio, W/H;
D,	hydraulic diameter;
f,	friction factor, $(-\mathrm{d}p/\mathrm{d}x)D/\frac{1}{2}\rho U^2$;
H,	channel height;
K,	dimensionless incremental pressure drop, equation (7);
$K(\infty)$,	fully developed value of K;
p,	static pressure;
p_0,	upstream stagnation pressure;
Re,	Reynolds number, UD/ν;
U,	mean velocity;
W,	channel width;
x,	axial coordinate;
ν,	kinematic viscosity;
ρ,	density.

INTRODUCTION

THE HYDRODYNAMIC development of laminar duct flows is a basic problem in internal fluid mechanics. The analysis of such flows has been primarily confined to elementary duct configurations such as the circular tube and the parallel-plate channel, wherein the cross sectional dependence of the velocity field can be specified by a single coordinate. For more general duct shapes, where two cross sectional coordinates are required in the specification of the velocity field, the available analytical solutions involve various degrees of approximation and are limited to selected rectangular and triangular cross sectional geometries. Experimental information on developing laminar duct flows is remarkably sparse, with the reported measurements being primarily for the circular tube.

The present research constitutes a comprehensive experimental investigation of laminar flow development in rectangular ducts, encompassing the range of cross section aspect ratios from 1:1 (square duct) to 51:1 (near approximation to a parallel-plate channel). The Reynolds numbers of the experiments ranged from 400 to 3000. To facilitate so broad an investigation, a highly flexible apparatus was employed which permits the synthesis of rectangular ducts of any aspect ratio. In particular, to obtain development

regions of suitable length and pressure gradients of sufficient magnitude to permit highly accurate measurements, it was found advantageous to make use of ducts of different cross sectional dimensions having a common aspect ratio. To meet the objectives of the research, seventeen different ducts were employed during the course of the experiments. The working fluids were distilled water and a light oil, the latter selected to facilitate measurements in the range of lower Reynolds numbers.

The major concern of the present research is with the pressure field associated with the hydrodynamic development of the flow. Information on the developing pressure field is presented in terms of axial pressure distributions and in terms of the incremental pressure drop due to the flow development. Fully developed values of the latter quantity, which correspond to the completion of the flow development process, are also given. On the basis of these results, Reynolds numbers are identified below which there are significant contributions of the viscous normal stresses. The experimental findings are compared with available predictions of analysis, thereby providing insights into the influence of the approximations involved in the analytical models. Comparisons are also made with the limited experimental information reported in the literature.

Prior contributions that are relevant to the present investigation will now be reviewed briefly. Measurements of the developing pressure field in rectangular ducts appear to have been limited to aspect ratios of 2:1 and 5:1 [1], with the data for the 2:1 duct being of uncertain validity owing to the possible presence of secondary flow. Fully developed values of the incremental pressure drop in a 3:1 duct are reported by Irvine and Eckert [2].

The published analyses of the flow development in rectangular ducts of finite aspect ratio have incorporated linearized forms of the inertia terms as well as assumptions about the relative magnitudes of the various viscous terms and about the cross sectional uniformity of the pressure (Han [3], Fleming and Sparrow [4], and Wiginton and Dalton [5]). The linearization employed by Han is basically different from that employed by Fleming and Sparrow and by Wiginton and Dalton; the methods of the latter pair of investigations differ from each other in lesser details which, nevertheless, lead to differences in the numerical results. Lundgren and co-workers [6] have devised a technique for predicting fully developed values of the incremental pressure drop for ducts of arbitrary cross sectional shape and have made application to rectangular ducts of various aspect ratios.

More extensive analytical study has been accorded the parallel-plate channel. A variety of solution methods has been employed, including linearization of inertia terms (Han [3], Sparrow *et al.* [7]); series expansion (Collins and Schowalter [8]); integral momentum balance (Schiller [9]); and finite differences (Bodoia and Osterle [10]). These references are representative of the available publications.

EXPERIMENTAL APPARATUS

The experiments were carried out in a closed loop fluid flow facility which, as shown in Fig. 1, included along the path of flow, the test section, downstream plenum chamber, metering station, reservoir, pump, filter and upstream plenum chamber. A description of these components is given in the following paragraphs.

Test section. The test section is the heart of the experimental facility. It was designed and fabricated to facilitate the synthesis of rectangular ducts of any aspect ratio while maintaining dimensional tolerances to a high degree of precision. A schematic cross sectional view of the structure of the test section is shown in Fig. 2 (a). As is pictured therein, the test section consisted of four members, the upper and lower walls a and b, which were common to all ducts, and replaceable side walls c. The side walls were fabricated to extremely close tolerances (to within 0·0001 in.), and both members of a given set had identical dimensions. The dimensions H and W of the duct could be varied at will by

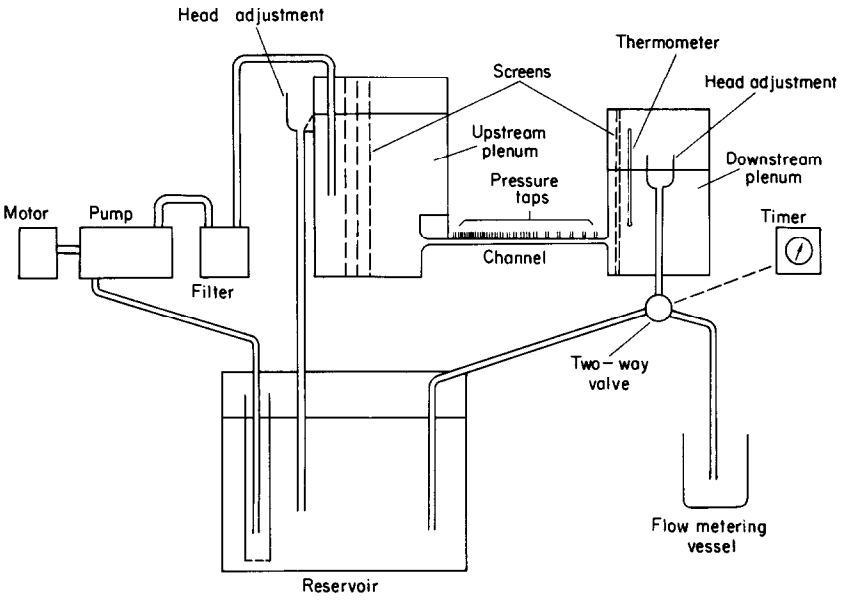

FIG. 1.

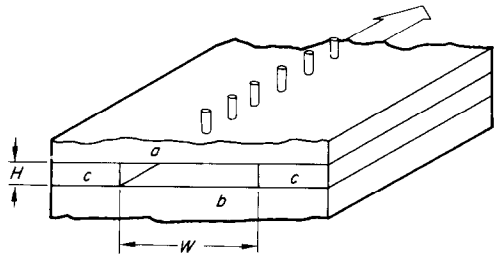

FIG. 2a.

employing side walls of different height and different lateral separation. In all, seventeen ducts encompassing eight aspect ratios ranging from 1:1 to 51:1 were employed, and these are listed in Table 1. All ducts were approximately $16\frac{1}{2}$ in. in length.

The upstream extremities of the duct walls were designed to provide a separation-free contraction from the upstream plenum to the duct proper. The contraction was accomplished by means of a quarter ellipse with major and minor axes of 1 in. and 0·5 in. respectively, see Fig. 2 (b), this shape being based on the results of Rouse and Hassan [11]. The quarter ellipse

Table 1. *Aspect ratios and duct dimensions*

Aspect ratio A	H (in.)	W (in.)
1	0·2502	0·2500
1	0·1000	0·1000
1·3	0·0808	0·1062
2	0·2502	0·5000
2	0·1993	0·3984
2	0·1260	0·2500
2	0·0627	0·1254
5	0·1540	0·7700
5	0·1895	0·9476
5	0·1000	0·5000
10	0·1540	1·5400
10	0·1890	1·8950
10	0·0627	0·6250
20	0·1540	3·0800
20	0·0627	1·2500
28	0·0637	1·8000
51	0·0627	3·2000

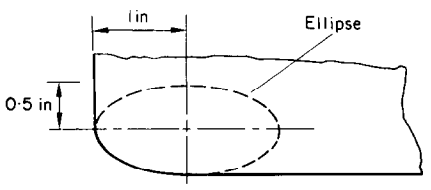

FIG. 2b.

contour was machined into all four walls of all of the ducts employed in the experiments.

The lower wall and the side walls of the ducts were fabricated from aluminium, and the surfaces which bounded the flow were polished to a high degree of smoothness. The upper wall was made from an optically flat, ground glass plate. Pressure taps, formed from 0·031 in. i.d. brass tubing, were installed along the length of the upper wall, see Fig. 2 (a), and lapped flush with the glass. Twenty-eight such pressure taps were distributed along the length of the duct, with a closer spacing between taps situated in the upstream portion of the duct.

The distribution of static pressure along the test section was displayed on a glass tube manometer bank. The liquid levels were read with a Gaertner cathetometer capable of discriminating heights to within 0·05 mm (0·002 in.).

Other elements of the experimental apparatus. The upstream plenum served the dual function of a flow control device and a calming chamber. The liquid level could be set and maintained at any desired height by means of an overflow weir which was adjustable to any vertical position. Accordingly, the upstream plenum functioned as a constant head tank. Calming was accomplished by the substantial volume of the plenum and by three stainless steel screens. A static pressure tap was situated in the wall of the plenum to provide a reference value for the static pressures measured in the test section.

The downstream plenum was also fitted with an overflow weir that could be arbitrarily positioned so as to fix the liquid level in the plenum at any desired height. Independent adjustment of the overflow weirs in the upstream and downstream plenums thus permitted specification of the pressure difference between the inlet and outlet cross sections of the test section.

Upon leaving the downstream plenum, the working fluid passed through a two-way valve, one outlet of which led to the flow metering station while the other outlet led to the reservoir. Metering was performed by direct weighing of quantities of working fluid, typically of the order of 4000 g. For this purpose, a precision beam balance was employed which could be read to 0·1 g. The time required to accumulate the weighed samples was measured by a timer driven by a synchronous electric motor, the timer being automatically actuated by the flow control valve. The timer could be read to 0·05 s.

Except for those periods devoted to metering, the flow was normally ducted to the reservoir, from whence it passed to the pump, which employed a novel rotating screw action to provide a steady continuous discharge. A 5μ filter was situated in the line between the pump outlet and the upstream plenum.

Working fluids. Two fluids, distilled water and a light oil, were employed during the course of the experiments to cover the higher and lower Reynolds number ranges respectively. The selection of the oil was made on the basis of its viscosity, the objective being to perform accurate measurements in the Reynolds number range from approximately 400 to 1000. The viscosity of the oil was measured over a range of temperatures with a Fenske viscometer, the calibration of which was checked against a standardized calibrating fluid. For example, at 70°F, the absolute viscosity of the oil was 6·36 times that of water and its specific gravity was 0·831. All experiments were performed in a laboratory room in which the temperature was maintained approximately constant at 70°F.

RESULTS AND DISCUSSION

As a prelude to the presentation and discussion of the results, attention is first turned to the determination of the effective starting point of the hydrodynamic development. Subsequent subsections then deal with axial pressure distributions, axial variations of the incremental pressure drop, and fully developed values of the incremental pressure drop. These sections will include comparisons with available analytical and experimental information.

Effective start of the hydrodynamic development. In analytical treatments of hydrodyn-

amically developing duct flows, it is generally postulated that the velocity is uniform across the inlet section of the duct. On the other hand, in both experimental research and engineering practice, the velocity profile at the initial cross section of the duct is, in general, not uniform, but rather is dependent on the geometry of the transition section between the plenum and the duct.* In particular, with a contoured contraction such as that employed here, Fig. 2 (b), there is an inevitable boundary layer development in the transition section, with a resulting nonuniformity in the velocity profile at the initial cross section of the duct. Fortunately, owing to the rapid acceleration of the flow, the boundary layer growth in the transition section is held in check, so that, as in the present experiments, the hydrodynamic development in the duct may be only slightly affected.

It is worthwhile to rationalize the conditions of analysis and of experiment so as to permit a more meaningful comparison of results. In addition, to give greater generality to the experimental findings, it is appropriate to uncouple the results for the hydrodynamically developing duct flow from the influence of the transition section. In pursuing these objectives, a procedure is employed which is similar in spirit to that generally used in interpreting experimental data for external boundary layer flows; that is, an effective starting point for the flow field development is sought. Although the resulting shifts in the streamwise coordinate were found to have only a very small influence on the present results, it is of interest to describe and illustrate the technique for finding the effective start of the hydrodynamic development.

In the present experiments, the position of the effective starting point was determined in accordance with the criterion

$$\frac{p_0 - p}{\frac{1}{2}\rho U^2} = 1 \tag{1}$$

in which p_0 is the stagnation pressure (i.e. in the upstream plenum), p is the local static pressure in the duct, ρ is the fluid density, and U is the mean velocity. Equation (1) is also satisfied by the analytical model of a cross sectionally uniform inlet velocity profile, and this is the rationale for its application here.

The technique for implementing the application of equation (1) is as follows. From the theory of the flow development in a parallel-plate channel [12], it can be reasoned that in the near neighborhood of the initial cross section of a rectangular duct, where there is negligible interaction between the wall boundary layers, the axial distribution of the static pressure should be expressible as

$$\frac{p_0 - p}{\frac{1}{2}\rho U^2} = 1 + C_1 x^{\frac{1}{2}} \tag{2}$$

in which $x = 0$ corresponds to the condition $(p_0 - p)/\frac{1}{2}\rho U^2 = 1$, and C_1 is a constant. Next, we consider a linear shift of the streamwise coordinate so that $x = x' + \xi$. With this, and with the introduction of the hydraulic diameter D and the Reynolds number Re

$$D = \frac{4HW}{2(H + W)}, \qquad Re = \frac{UD}{\nu} \tag{3}$$

equation (2) can be rephrased as

$$\left[\frac{p_0 - p}{\frac{1}{2}\rho U^2} - 1\right]^2 = C_2 \frac{x'/D}{Re} + C_3. \tag{4}$$

Provided that the reasoning leading to equation (2) is valid, a graph of experimentally determined values of

$$\left[\frac{p_0 - p}{\frac{1}{2}\rho U^2} - 1\right]^2$$

plotted as a function of $(x'/D)/Re$ should yield a straight line, at least in the near neighborhood of the initial cross section of the duct. Furthermore, the intercept of such a straight line on the abscissa axis indicates the shift in the streamwise coordinate, to be added to or subtracted from $(x'/D)/(Re$, which locates $x = 0$ at the cross section at which $(p_0 - p)/\frac{1}{2}\rho U^2 = 1$.

* A similar gulf between the idealizations of analysis and the realities of experiment is encountered in external boundary layer flows, specifically, in connection with the geometry of the leading edge.

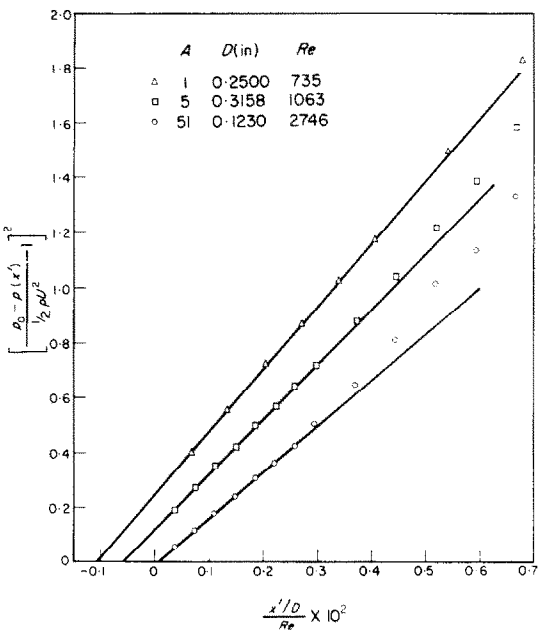

FIG. 3.

Figure 3 has been prepared to illustrate the aforementioned relationships. The figure shows data from three representative experiments, the corresponding operating conditions being listed in the upper part of the figure. The plotted points represent pressure measurements in the upstream portion of the duct, adjacent to the initial cross section. The origin of x' is situated in the transition section, just upstream of the initial cross section of the duct.

The figure shows that the experimental data are in complete accord with the linear relationship expressed by equation (4), thereby verifying the model underlying its derivation. As is to be expected, the linear relationship ceases to be valid at larger downstream distances. For the majority of the experiments, it was found that the abscissa intercepts fell at $x' < 0$. In those few cases where the intercepts fell at $x' > 0$, the departures from $x = 0$ were exceedingly small. These findings, taken together with the fact that $x' = 0$ is, itself, a point situated just upstream of the initial cross section of the duct, indicate that the condition $(p_0 - p)/\frac{1}{2}\rho U^2 = 1$ occurs in the transition section. This state of affairs is physically reasonable.

In the forthcoming presentation of results, the origin of the streamwise coordinate x will be identified with the point at which $(p_0 - p)/\frac{1}{2}\rho U^2 = 1$. As was noted earlier, the shift in the origin of the streamwise coordinate from the initial cross section of the duct to that defined above has a very small effect on the final results.

Axial pressure distributions. The results for the developing pressure field can be presented in several forms, the most direct being the axial pressure distribution itself. On the other hand, from the standpoint of a more concise representation of the results, a presentation in terms of the incremental pressure drop is more suitable. In addition, the use of the incremental pressure drop facilitates the identification of the conditions marking the onset of fully developed flow. Representative results for the axial pressure field, encompassing three duct aspect ratios, will be presented in this subsection. A more complete presentation of results, in terms of the incremental pressure drop, is made in subsequent subsections.

Axial pressure distributions for aspect ratios A of 1, 5 and 51, are given respectively in Figs. 4 (a)–4 (c). In each figure, the local pressure defect $(p_0 - p)$, normalized by the dynamic pressure $\frac{1}{2}\rho U^2$, is plotted as a function of the dimensionless streamwise coordinate $(x/D)/Re$. The data points are distinguished according to Reynolds number. In the interests of clarity, available data for other Reynolds numbers have not been included in these figures.

Inspection of the figures indicates that the pressure defect increases rapidly in the upstream portion of the duct, owing to the combined effects of momentum change and large wall shear stress. With increasing downstream distances, the increase in the pressure defect becomes more gradual, ultimately becoming a linear function of the streamwise coordinate. At fixed values of $(x/D)/Re \leqslant 0{\cdot}01$, the dimensionless pressure defect decreases very slightly with increasing aspect

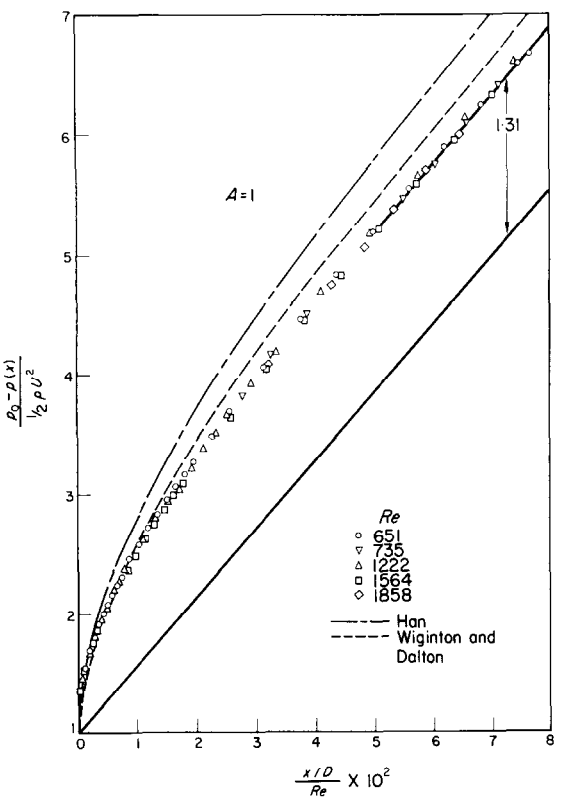

FIG. 4a.

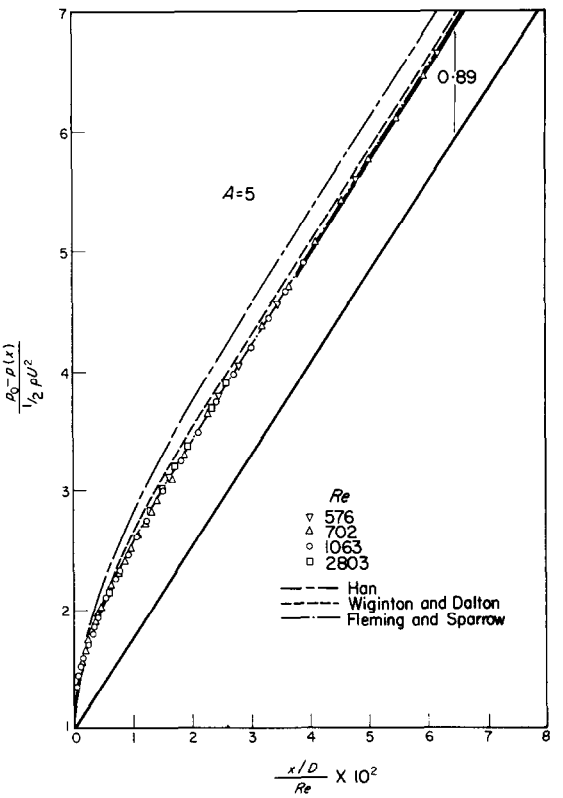

FIG. 4b.

ratio. On the other hand, an opposite and stronger variation is in evidence at larger values of $(x/D)/Re$.

Within the range dealt with in the figures, the use of $(x/D)/Re$ as the abscissa variable appears to successfully remove the Reynolds number as a separate parameter. Further remarks will be made later about the role of the Reynolds number.

In addition to the experimental data, Figs. 4 (a)–4 (c) contain several curves, the significance of which will now be discussed. In each figure, there is a straight line passing through the origin and sloping upward to the right, the equation of which is

$$\frac{p_0 - p(x)}{\frac{1}{2}\rho U^2} = 1 + (f \,.\, Re)\frac{x/D}{Re} \qquad (5)$$

where

$$f \,.\, Re = \frac{128A^3/(1 + A^2)}{\frac{4}{3}A - 8\sum_{n=0}^{\infty} \frac{\tanh\,[(2n + 1)\pi A/2]}{[(2n + 1)/(\pi/2)]^5}}. \qquad (6)$$

These lines represent the dimensionless pressure defect for a flow which is hydrodynamically developed right from $x = 0$, and $f \,.\, Re$ is the friction factor, Reynolds number product for hydrodynamically developed flow.* In Fig. 4 (c), two such straight lines are shown, one for $A = 51$

* The experimentally determined $f \cdot Re$ values were typically within one per cent of the theoretical values given by equation (6). This level of agreement lends confidence to the experimental technique and implies the absence of secondary flow.

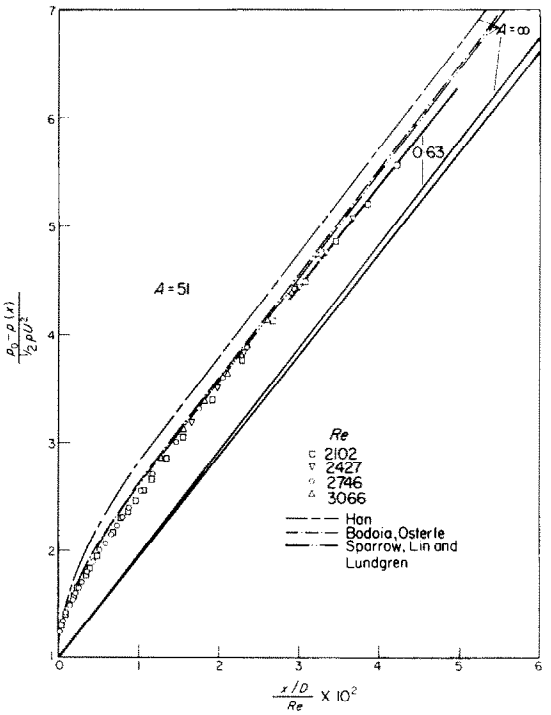

FIG. 4c.

and the second for $A = \infty$ (parallel-plate channel).

The vertical displacement of the experimental data from the aforementioned straight lines corresponds to the (dimensionless) incremental pressure drop due to the hydrodynamic development of the flow. For any given duct, the incremental pressure drop increases with increasing downstream distance, ultimately taking on a constant value in the region of developed flow. At a fixed $(x/D)/Re$, smaller incremental pressure drops are sustained by ducts of higher aspect ratio.

The magnitude of the fully developed incremental pressure drop is indicated at the right margin of each figure; more will be said later about the determination of these values.

The other curves appearing in the figures represent the predictions of analysis. Inasmuch as there are no analytical results available for a duct aspect ratio of 51 [Fig. 4(c)], the analytical predictions for the parallel-plate channel ($A = \infty$) are shown instead.

The pressure defect results of Han [3] are generally higher than those of experiment. Wiginton and Dalton's predictions [5] are also somewhat higher than the data, but to a lesser extent than Han. On the other hand, the analytical results of Fleming and Sparrow [4] are in excellent accord with experiment. Also, if

allowance is made for differences between $A = 51$ and $A = \infty$, then the predictions of Bodoia and Osterle [10] and of Sparrow *et al.* [7] may be regarded as being in satisfactory agreement with the data.

All of the above-mentioned analyses, except for Bodoia and Osterle's finite-difference solution for the parallel-plate channel, make use of linearized forms of the inertia terms. Han's model differs in a fundamental way from the others and, at least from the standpoint of Figs. 4 (a)–4 (c), appears to be more approximate. The other analyses start with the same basic linearization, but there are subsequent differences in detail between the solution methods of Wiginton and Dalton and of Fleming and Sparrow. In addition, the latter investigators employed a much larger number of terms in their numerical evaluations than did the former. The comparisons shown in Figs. 4 (a)–4 (c) appear to favor the Fleming and Sparrow results.

Incremental pressure drop distributions. The concept of the incremental pressure drop due to flow development has already been introduced in the preceding subsection. If the dimensionless incremental pressure drop is denoted by $K(x)$, then one has the defining equation

$$K(x) = \frac{p_0 - p(x)}{\frac{1}{2}\rho U^2} - \left[1 + (f \,.\, Re)\frac{x/D}{Re}\right] \quad (7)$$

in which $f \,.\, Re$ denotes the friction factor, Reynolds number product for fully developed flow, equation (6). Thus, in accordance with equation (7), values of $K(x)$ are determined by subtracting a linear component, which corresponds to a flow which is fully developed right from $x = 0$, from the local pressure defect $(p_0 - p)/\frac{1}{2}\rho U^2$. On the other hand, if the axial distribution of $K(x)$ is given, the local pressure defect is found by simple addition.

Axial distributions of the incremental pressure drop are presented in Figs. 5 (a)–5 (d). These figures encompass eight aspect ratios ranging from $A = 1$ to $A = 51$, the successive figures

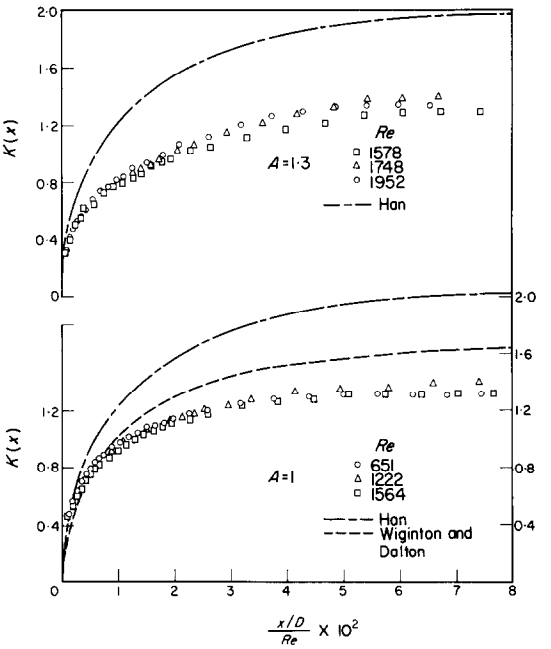

FIG. 5a.

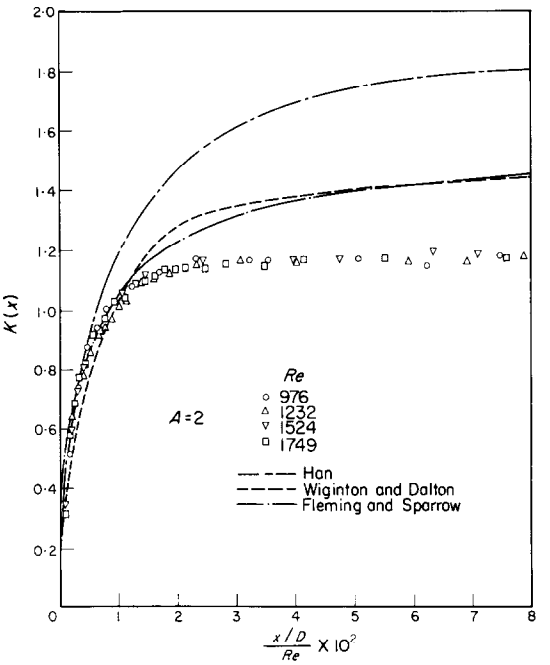

FIG. 5b.

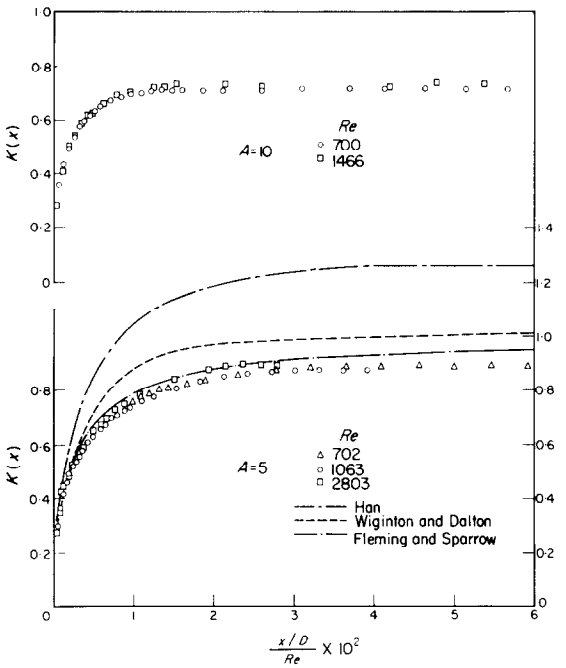

FIG. 5c.

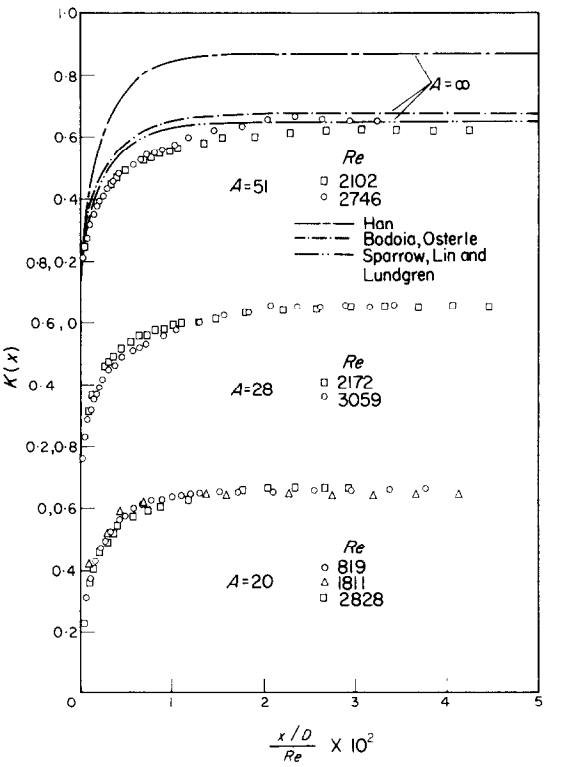

FIG. 5d.

being arranged in order of increasing aspect ratio. To preserve the clarity of the figures, only data for representative Reynolds numbers are included. In addition to the experimentally determined $K(x)$ distributions, Figs. 5 (a)–5 (d) also contain curves which represent the predictions of analysis.

From the figures, it is seen that the axial distribution of K has a form that is common to ducts of all aspect ratios. At $x = 0$, K is zero in accordance with its definition, equation (7). With increasing downstream distance, K rises sharply at first and then tends to level off, ultimately taking on a constant value characteristic of the fully developed regime. This behavior is entirely consistent with the interpretation of $K(x)$ as the *accumulated* increment in the pressure drop due to flow development between $x = 0$ and $x = x$. Thus, in the region of hydrodynamic development, K necessarily increases with increasing x. On the other hand, when the hydrodynamic development is complete, there are no further contributions to K and a constant value is attained. This constant value corresponds to the overall incremental pressure drop due to the entire flow development process.

In interpreting the level of agreement between the experimental results and the predictions of analysis, it is relevant to note that differences are accentuated by the subtractive process used to determine K. In other words, what may appear to be substantial deviations in K are of lesser significance in $(p_0 - p)/\frac{1}{2}\rho U^2$. In this light, a comparison of analytical and experimental results in Figs. 5 (a)–5 (d) yields conclusions identical to those already discussed in connection with Figs. 4 (a)–4(c).

The aforementioned subtractive process also tends to accentuate whatever scatter may be present amongst the data. Notwithstanding this, the data of Figs. 5 (a)–5 (d) may be regarded as being relatively free of scatter, especially com-

pared with that of similar experiments. Within the range of the figures, there are no evident trends with Reynolds number.

The length of the hydrodynamic development region may be defined in terms of the distance required for $K(x)$ to approach to within a preassigned percentage of its fully developed value. If a 95 per cent approach is stipulated, then the development length may be characterized as follows. For ducts having aspect ratios on the order of one, $(x/D)/Re = 0{\cdot}03$. The dimensionless development length decreases rapidly between $A = 1$ and 2 and thereafter remains relatively independent of aspect ratio, so that for ducts having aspect ratios $A \geqslant 2$, $(x/D)/Re = 0{\cdot}015$.

in which $K(\infty)$ is a constant which depends only on the aspect ratio A, and $f \,.\, Re$ is given by equation (6). The quantity $K(\infty)$ may be termed the fully developed incremental pressure drop. In view of the computational simplicity of equation (8), the numerical values of $K(\infty)$ appearing therein are of practical interest.

The experimentally determined $K(\infty)$ values are displayed in Fig. 6. The figure is divided into 9 graphs to accommodate the 8 aspect ratios of the present investigation and the experimental results of Irvine and Eckert [2] for a duct of aspect ratio 3. The abscissa variable is the Reynolds number, and data points are shown for all of the Reynolds numbers investigated. On

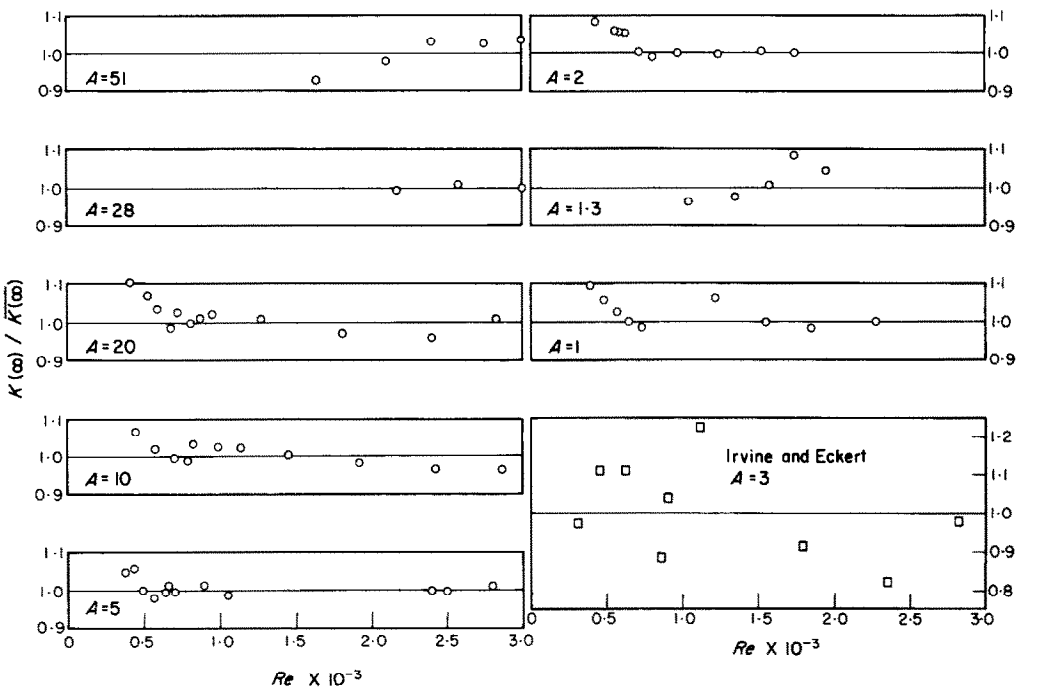

FIG. 6.

Fully developed K *values.* At axial positions downstream of the development region, the pressure defect $p_0 - p$ is calculable from

$$\frac{p_0 - p(x)}{\frac{1}{2}\rho U^2} = K(\infty) + 1 + (f \,.\, Re)\frac{x/D}{Re} \qquad (8)$$

each ordinate is plotted $K(\infty)/\overline{K(\infty)}$, where $K(\infty)$ corresponds to the Reynolds numbers of the abscissa and $\overline{K(\infty)}$ is a mean value specific to each aspect ratio A. The mean value is taken over those Reynolds numbers where the effects of viscous normal stresses appear to be absent

(such stresses are accentuated at low Reynolds numbers).

Aside from systematic deviations at low Reynolds numbers, the present data show only minimal scatter, especially when compared with that of the Irvine–Eckert data, the scatter of which is typical of other investigations of this type.

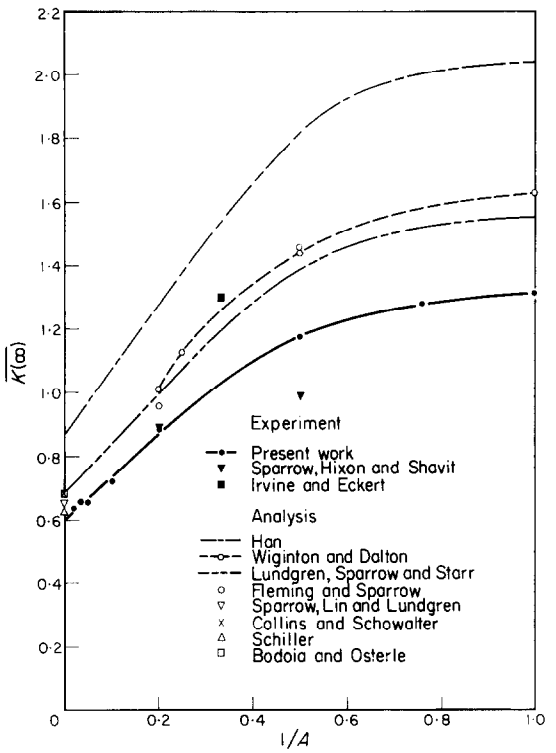

FIG. 7.

On the basis of Fig. 6, it can be safely concluded that $K(\infty)$ is independent of Reynolds number, provided that the Reynolds number is sufficiently large. However, at lower Reynolds numbers, $K(\infty)$ increases as Re decreases, this increase being attributable to the effect of the viscous normal stresses. From an inspection of Fig. 6, it appears that these viscous effects can be neglected for Reynolds numbers above 500–600.

Values of $\overline{K(\infty)}$ from the present experiments are given in Fig. 7 along with the results of analysis* and of other experimental investigations. To facilitate a compact presentation, $\overline{K(\infty)}$ is plotted as a function of the reciprocal aspect ratio $1/A$. It is seen from this figure that there is general concurrence in the trend that $\overline{K(\infty)}$ increases as the aspect ratio decreases; that is, the highest value of $\overline{K(\infty)}$ is attained for a duct having a square cross section.

In appraising the comparisons shown in Fig. 7, it should be noted that an uncertainty of 0·1–0·2 in $K(\infty)$ does not induce substantial errors in the dimensionless pressure defect $(p_0 - p)\frac{1}{2}\rho U^2$. Among the analytical predictions, those of Lundgren *et al.* [6] are in closest accord with the experimental data. This finding is of practical significance inasmuch as the aforementioned analytical method yields $K(\infty)$ values for ducts of arbitrary cross sectional shape without having to solve for the hydrodynamic development of the flow.

In general, there is better agreement between analysis and experiment for ducts of large aspect ratio than for ducts of small aspect ratio. This finding is consistent with the fact that fewer approximations are required in the analysis of a parallel-plate channel than in the analysis of a duct of finite aspect ratio.

Finally, turning to the results of other experiments, it is seen that the $A = 5$ point of Sparrow *et al.* [1] is in virtually exact agreement with the present value, while that for $A = 2$ falls low. The latter point is of uncertain validity owing to the possible presence of secondary flow. On the other hand, the Irvine–Eckert point falls somewhat high, but the considerable data scatter experienced in that investigation (see Fig. 6) is suggestive of some uncertainty in accuracy.

ACKNOWLEDGEMENT

The support of this research by the National Science Foundation under grant GK-1876 is gratefully acknowledged.

* All of the analyses neglect the effect of the viscous normal stresses.

REFERENCES

1. E. M. SPARROW, C. W. HIXON and G. SHAVIT, Experiments on laminar flow development in rectangular ducts, *J. Basic Engng* **89**, 116–124 (1967).
2. T. F. IRVINE, JR. and E. R. G. ECKERT, Comparison of experimental information and analytical prediction for laminar entrance region pressure drop in ducts with rectangular and triangular cross sections, *J. Appl. Mech.* **25**, 288–290 (1958).
3. L. S. HAN, Hydrodynamic entrance lengths for incompressible laminar flow in rectangular ducts, *J. Appl. Mech.* **27**, 403–409 (1960).
4. D. P. FLEMING and E. M. SPARROW, Flow in the hydrodynamic entrance region of ducts of arbitrary cross section, *J. Heat Transfer* (in press).
5. C. L. WIGINTON and C. DALTON, Incompressible laminar flow in the entrance region of a rectangular duct, *12th Int. Congr. Appl. Mech.*, Stanford University, Stanford, California, August, 1968.
6. T. S. LUNDGREN, E. M. SPARROW and J. B. STARR, Pressure drop due to the entrance region in ducts of arbitrary cross section, *J. Basic Engng* **86**, 620–626 (1964).
7. E. M. SPARROW, S. H. LIN and T. S. LUNDGREN, Flow development in the hydrodynamic entrance region of tubes and ducts, *Physics Fluids* **7**, 338–347 (1964).
8. M. COLLINS and W. R. SCHOWALIER, Laminar flow in the inlet region of a straight tube, *Physics Fluids* **5**, 1122–1124 (1962).
9. L. SCHILLER, Die Entwicklung der laminaren Geschwindigkeitsverteilung und ihre Bedeutung für Zähigkeitmessungen, *ZAMM* **2**, 96–106 (1922).
10. J. R. BODOIA and J. F. OSTERLE, Finite difference analysis of plane Poiseuille and Couette flow developments, *Appl. Sci. Res.* **A10**, 265–276 (1961).
11. H. ROUSE and M. M. HASSAN, Cavitation-free inlets and contractions, *Mech. Engng* **71**, 213–216 (1949).
12. H. SCHLICHTING, *Boundary Layer Theory*, 6th edn. McGraw-Hill, New York (1968).

EXPÉRIENCES SUR L'ÉCOULEMENT PENDANT L'ÉTABLISSEMENT DU RÉGIME HYDRODYNAMIQUE DANS DES CONDUITS RECTANGULAIRES D'ALLONGEMENT ARBITRAIRE

Résumé—Une vaste étude expérimentale de l'établissement de l'écoulement laminaire dans des conduits rectangulaires est effectuée en employant un appareil qui permet l'étude de n'importe quel allongement de la section droite. Le premier souci de la recherche est la détermination du champ de pression associé avec l'établissement hydrodynamique de l'écoulement. Les résultats expérimentaux sont présentés en fonction à la fois de la différence locale de pression et de la chute de l'augmentation de pression due à l'établissement de l'écoulement. Des comparaisons sont faites avec les prévisions théoriques disponibles et avec les renseignements expérimentaux antérieurs. Les longueurs d'établissement hydrodynamique sont déduites et le seuil des effets importants sur la contrainte normale visqueuse est identifié.

VERSUCHE ÜBER DEN HYDRODYNAMISCHEN EINLAUF IN RECHTECKKANÄLEN BELIEBIGER GRÖSSENVERHÄLTNISSE

Zusammenfassung—Es wurde eine umfassende experimentelle Untersuchung der Ausbildung laminarer Strömung in rechteckigen Kanälen durchgeführt. Dabei wurde eine Apparatur verwendet, die die Untersuchung jedes Richtungsverhältnisses im Querschnitt erlaubt. Das Ziel der Untersuchung ist die Bestimmung des Druckfeldes, welches sich bei der hydrodynamischen Ausbildung der Strömung einstellt. Die experimentellen Ergebnisse sind dargestellt, sowohl in Abhängigkeit des örtlichen Druckabfalls, als auch in Abhängigkeit der Zunahme des Druckabfalls durch die Ausbildung der Strömung. Die Ergebnisse werden verglichen mit vorhandenen analytischen Aussagen und mit früheren experimentellen Ergebnissen. Die hydrodynamischen Einlauflängen werden abgeleitet und die Grenze des merklichen Einflusses der Normalspannung der Viskosität wird festgestellt.

ЭКСПЕРИМЕНТАЛЬНОЕ ИССЛЕДОВАНИЕ ГИДРОДИНАМИЧЕСКОГО РАЗВИТИЯ ТЕЧЕНИЯ В ПРЯМОУГОЛЬНЫХ КАНАЛАХ С ПРОИЗВОЛЬНЫМ ОТНОШЕНИЕМ СТОРОН

Аннотация—Экспериментально исследуется развитие ламинарного течения в прямоугольных каналах на установке, позволяющей проводить эксперименты при любом соотношении сторон. Основное исследование сводится к определению поля давлений, связанного с гидродинамическим развитием потока. Экспериментальные резульсаты представлены в виде локального дефекта давления и инкрементного падения давления за счет развития нотока. Полученные результаты сравниваются с имеющимися теоретическими и экспериментальными данными. Найдены длины гидродинамических начальных участков, а также установлен предел значительных влияний вязкого нормального напряжения.